Stimulated Raman amplification of femtosecond pulses in hydrogen gas

V. Krylov*, A. Rebane, D. Erni, O. Ollikainen,† and U. Wild

Physical Chemistry Laboratory, Swiss Federal Institute of Technology, ETH-Zentrum, CH-8092 Zurich, Switzerland

V. Bespalov and D. Staselko

S. I. Vavilov State Optical Institute, St. Petersburg, Russia 199034

Received May 7, 1996

We report efficient amplification of weak femtosecond supercontinuum pulses by a stimulated Raman scattering process in pressurized H_2 gas excited with 350-fs-duration frequency-doubled pulses from a regenerative-amplified Ti:sapphire laser. An amplification factor of 10^9 is obtained at the wavelength of 465 nm for seed pulses produced by supercontinuum generation in glass. © 1996 Optical Society of America

Stimulated Raman scattering (SRS) is a well-known method for frequency conversion of laser radiation, including femtosecond laser pulses.[1–6] However, because the SRS process starts from fluctuations of quantum noise[7] it is usually a difficult task to optimize simultaneously the energy conversion efficiency, the spatial beam quality, and the stability of the output Stokes field. By using stimulated Raman amplification (SRA) of a seed signal, one can reduce the pumping threshold and considerably improve the parameters of the output beam.[8–16] There have been numerous investigations of SRA in the quasi-steady-state regime in which nanosecond and subnanosecond excitation pulses were used.[8–12] Recently, experiments on SRA with picosecond excitation pulses were performed,[13–16] and it was shown that it is also useful to apply seeding to improve the parameters of the Stokes-shifted radiation in a transient regime.

Previous studies of femtosecond SRS have revealed several differences from SRS excited in the picosecond and nanosecond pulse regimes. It was observed that phenomena such as self-phase modulation and self-focusing can lower the efficiency of SRS.[3] Because the pulse duration is much shorter than the dephasing time of the Raman polarizability, more pump energy is needed to reach the threshold of SRS.[1,5] In addition, because of the broad spectral width of the femtosecond pulses, group-velocity mismatch can reduce the effective interaction length of the pump and the Stokes pulses.[6] Until now, the influence of these processes in seeded SRS has not been considered to our knowledge.

In this Letter we report on an experiment in which we study, for the first time to our knowledge, SRA on the femtosecond time scale. We show that efficient amplification of ultrashort signals is possible in a H_2 gas excited by frequency-doubled regenerative-amplified femtosecond Ti:sapphire laser pulses. We investigate, for the first time to our knowledge, SRA seeded with femtosecond supercontinuum pulses and demonstrate the use of SRA for time-resolved measurement of weak ultrafast signals.

A schematic of our experimental setup is shown in Fig. 1. The femtosecond laser source is a commercial 1-kHz repetition-rate Ti:sapphire regenerative-amplified laser system (CPA-1, Clark MXR). The duration of the output pulses at the fundamental wavelength of 780 nm is 200 fs, and the energy is 0.75 mJ/pulse. After the frequency is doubled in a 2.5-mm-thick KDP crystal we obtain 350-fs-duration pulses with 0.3-mJ energy at the 390-nm wavelength. The Raman amplifier consists of a stainless-steel 1-m-long cell filled with H_2 at pressure P of 45 bars. Under these conditions the dephasing time for the vibrational motion of H_2 molecules is $T_2 = 140$ ps.[17] We note that this relaxation time is much longer than the duration of the excitation pulses, which corresponds to a transient regime of the stimulated Raman process.

To produce a supercontinuum, we split off a small part of the fundamental beam and focus it on a glass plate.[18] The blue part of the supercontinuum

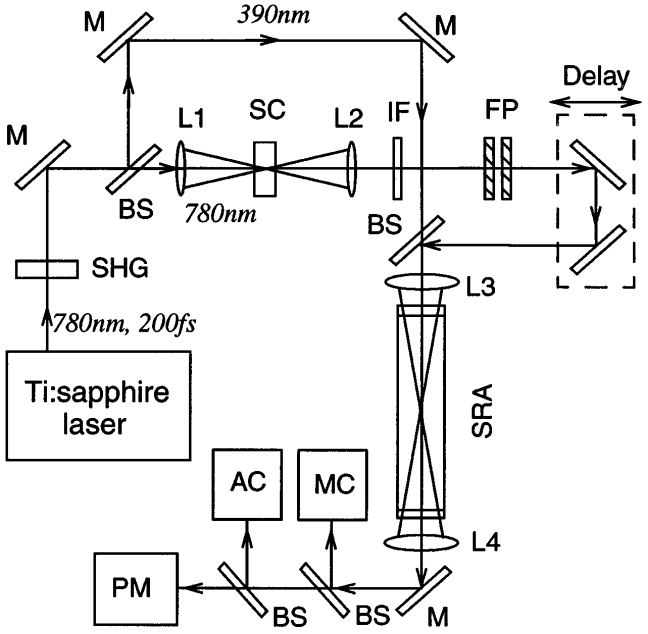

Fig. 1. Experimental setup: SHG, second-harmonic generation in KDP crystal; M's, mirrors; BS's, beam splitters; L1–L4, lenses; SC, glass plate for supercontinuum generation; IF, interference filter; FP, Fabry–Perot étalon; SRA, gas cell; AC, autocorrelator; PM, power-energy meter; MC, grating monochromator.

0146-9592/96/242005-03$10.00/0

radiation is collimated with a second lens and focused together with the 390-nm pump beam in the SRA cell by a 1-m focal-length lens (L3). Another 1-m focal-length lens (L4) collimates the radiation at the output of the cell. The delay between the pump and the seed pulses is controlled by an optical delay line. The duration of the seed pulses is 200 fs. To measure simultaneously the energy, the spectrum, and the duration of the pulses, we divide the beam at the output of the SRA cell among a power-energy meter, a grating monochromator, and an autocorrelator.

The first step of the experiment is to measure the dependence of the energy of the first Stokes component at the wavelength $\lambda = 465$ nm on the energy of the pump pulses at a fixed seed pulse energy. The energy of the seed after the interference filter was $\sim 10^{-6}$ μJ ($\lambda = 465$ nm, $\Delta\lambda = 10$ nm). The delay between the seed and the pump pulses was optimized for maximum SRA signal intensity. Figure 2 shows the measured Stokes pulse energy at the output versus the pump pulse energy at the input of the cell. Efficient amplification of the seed signal starts at a pump energy of ~ 15 μJ. At pump energy greater than 25 μJ the Raman signal intensity shows progressively less dependence on the presence of the seed, and at greater than 40 μJ a saturation of the energy of the first Stokes component is observed. The amplification factor K, defined as the ratio of the outgoing and the incoming pulse energies at the first Stokes wavelength, measured at the maximum pump energy of 100 μJ, is approximately 2×10^7. Figure 2 also presents the Stokes pulse energy measured under the same pumping conditions but without the seed, which corresponds to conventional SRS. The SRS process shows a higher pumping threshold of 30 μJ and a lower maximum conversion efficiency to the first Stokes of $\sim 8\%$, compared with the 18% efficiency obtained with SRA.

Figure 3 shows the spectrum of the first Stokes component obtained with and without the seed at a pump pulse energy of 90 μJ, well above the SRS threshold. Under these conditions the seeding increases not only the Stokes signal's peak intensity but also its spectral width. Comparing this result with the transmission function of the interference filter, we conclude that the observed spectral broadening is due to the high Raman gain that amplifies the spectral wings of the seed pulse.

The advantage of using the seed lies in the reduction of the threshold and in the increase of the maximum conversion efficiency by approximately a factor of 2. In addition, the seeded Raman process yields an improved pulse-to-pulse energy stability and a better spatial beam quality than conventional SRS in the same configuration.

Our next concern is to investigate in more detail the behavior of the SRA as a function of the seed pulse parameters. For this we insert into the seed beam a Fabry–Perot étalon that comprises two parallel mirrors with $R = 50\%$ at a distance of $d = 430$ μm from each other. This arrangement transforms each seed pulse into a train of 200-fs-duration pulses with a time interval of 2.9 ps. The first seed pulse in the train has an energy of 10^{-6} μJ. The energy of each subsequent pulse is smaller by a factor of 4.

Figure 4 shows the intensity of the first Stokes component seeded by different pulses in the train, which we measure by simply varying the time delay between the pump and the seed beam. We observe that the first and the second amplified pulses have an almost equal peak intensity. Because the seed pulses at the input of the Raman cell differ in energy by a factor of 4, the SRA process is close to saturation. On the other hand, for the seed pulses with lower energy, the amplification appears to be linear as the relative intensity of the SRA signal peaks approaches the expected ratio of 1:4. From these data we estimate the effective seed pulse saturation energy to be $\sim 10^{-8}$ μJ.

From the measured dependence of SRA signal intensity on the delay we can, in principle, obtain information about the temporal shape of the seed pulses. For seed pulse energy below the saturation limit the SRA trace corresponds to the cross-correlation function between the pump pulse and the seed pulse. At optimum pump pulse energy of 90 μJ the Raman amplification factor is $K = 10^9$, which allows us to detect seed pulses as low as 10^{-10} μJ, corresponding to ~ 1000 photons/pulse. This shows that the SRA can actually be used to characterize the duration and the

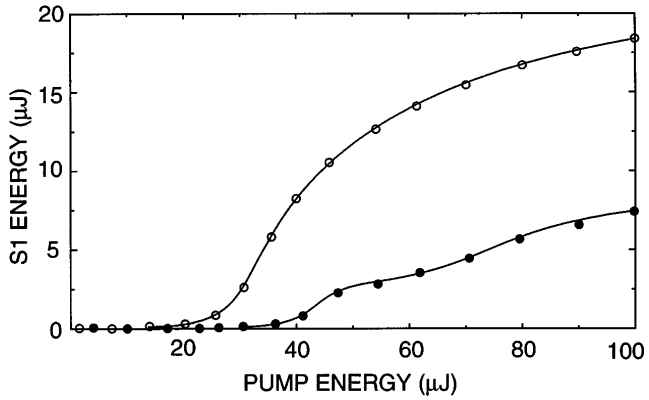

Fig. 2. Dependence of the energy of the first Stokes component (S1) on the energy of the pump pulses. Filled circles, S1 without seed; open circles, S1 with seed. The seed pulse energy is 10^{-6} μJ.

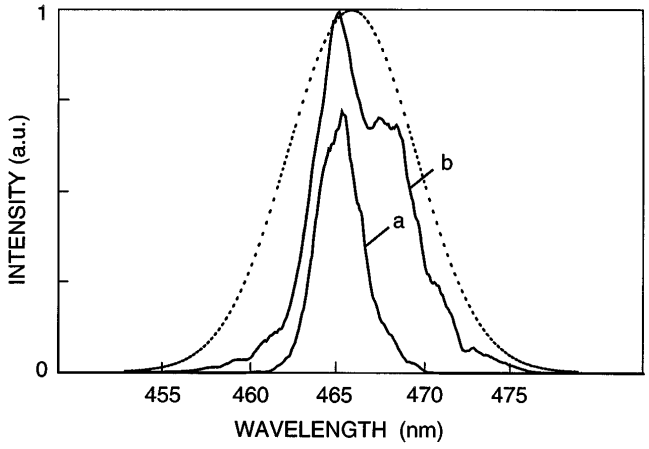

Fig. 3. Spectrum of the first Stokes (a) without seed and (b) with seed. The pump pulse energy is 90 μJ. Dotted curve, transmission spectrum of the interference filter.

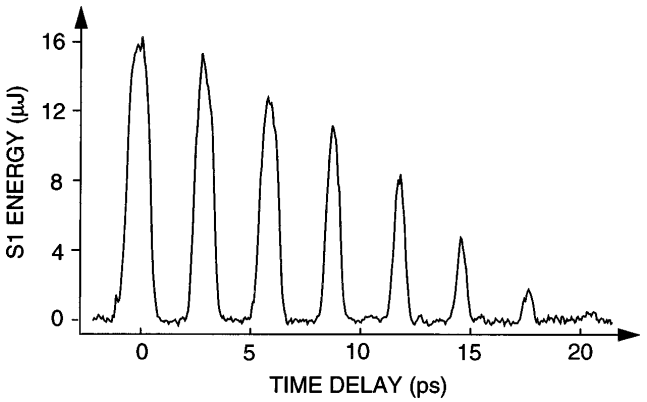

Fig. 4. Dependence of the first Stokes energy (S1) on the time delay between the pump pulse and the seed beam. The pump pulse energy is 90 μJ.

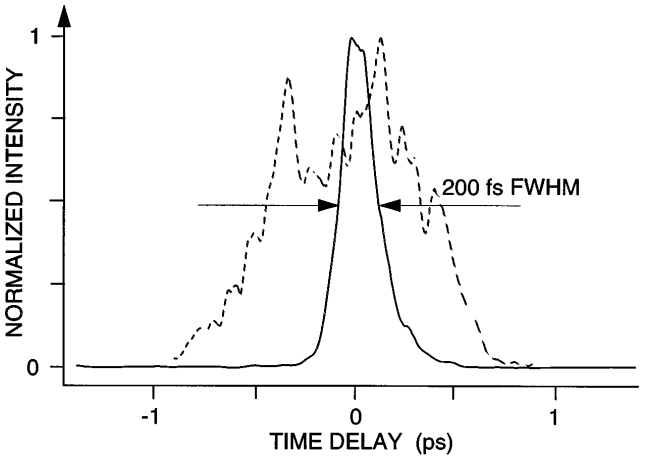

Fig. 5. Autocorrelation trace of the seeded Stokes pulse at seed energies of 10^{-6} μJ (dashed curve) and 10^{-9} μJ (solid curve).

shape of very weak femtosecond signals. At pulse energy greater than the saturation level, deviations from the shape of the actual cross-correlation function occur, as can be seen from the broadening of the SRA traces corresponding to more intensive seed pulses in Fig. 4.

Figure 5 presents the temporal profile of the SRA pulse at two different seed pulse energies. We perform the autocorrelation of the SRA pulse by use of the usual frequency-doubling technique in a 1-mm-thick β-barium borate crystal. The saturation of the SRA is manifested as a temporal broadening of the Raman pulse from 200 to 600 fs as the energy of the seed pulses increases from 10^{-9} to 10^{-6} μJ.

At high pump energy of more than 90 μJ and with maximum seed energy of $\sim 10^{-6}$ μJ we observe, besides the first Stokes component, the generation of other Raman components, ranging from the second anti-Stokes ($\lambda = 294$ nm) to the third Stokes ($\lambda = 759$ nm), all accompanied by satellite rotational components. The quality of these higher Stokes components is also improved by supercontinuum seed pulses. However, it should be noted that the seeding has to occur at the wavelength of the first Stokes component, rather than at any other Stokes or anti-Stokes wavelength. We study this aspect by placing different bandpass interference filters ($\Delta\lambda = 10$ nm) in the seed beam. When the filter is chosen such that the seed wavelength is centered at any other Raman wavelength, no SRA is observed. This can be explained by the fact that the generation of higher Stokes components is a multistage process that depends critically on the existence of the first Stokes component.

In conclusion, our results show that SRA seeded with supercontinuum pulses is a practicable method to widen the wavelength range of regenerative-amplified femtosecond Ti:sapphire lasers. SRA results in a better pulse-to-pulse stability and improved spatial beam structure of the frequency-shifted radiation not only of the first Stokes component but also for other Stokes and anti-Stokes wavelengths. Because of the high amplification factor of as much as 10^9 the stimulated Raman technique can be used to measure the time profile of low-energy ultrashort signals down to 10^{-16} J. In addition, a supercontinuum appears to be a convenient source of seed pulses, especially in comparison with other methods such as using a second SRS gas cell.

*Permanent address, S. I. Vavilov State Optical Institute, 199034, St. Petersburg, Russia.

†Permanent address, Institute of Physics, EE2400, Tartu, Estonia.

References

1. V. Krylov, A. Rebane, O. Ollikainen, D. Erni, U. Wild, V. Bespalov, and D. Staselko, Opt. Lett. **21,** 381 (1995).
2. Y. Irie and T. Imasaka, Opt. Lett. **20,** 2072 (1995).
3. J. K. Wang, Y. Siegal, C. Lu, and E. Mazur, J. Opt. Soc. Am. B **11,** 1031 (1994).
4. P. G. May and W. Sibbett, Appl. Phys. Lett. **43,** 624 (1983).
5. G. Hilfer and C. R. Menyuk, J. Opt. Soc. B **7,** 739 (1990).
6. S. A. Akhmanov, V. A. Vysloukh, and A. S. Chirkin, in *Optics of Femtosecond Laser Pulses* (American Institute of Physics, New York, 1992), pp. 165–176.
7. R. C. Swanson, P. R. Battle, and J. L. Carlsten, Phys. Rev. A **42,** 6774 (1990).
8. V. G. Bespalov, V. N. Krylov, D. I. Staselko, and V. N. Sizov, Opt. Spectrosc. (USSR) **63,** 742 (1987).
9. J. Ottusch and D. Rockwell, IEEE J. Quantum Electron. **QE-24,** 2076 (1988).
10. J. G. Wessel, K. S. Repasky, and J. L. Carlsten, Phys. Rev. A **53,** 1854 (1995).
11. M. Bashkansky and J. Reintjes, Opt. Commun. **83,** 103 (1991).
12. S. Wada, H. Moriwaki, A. Nakamura, and H. Tashiro, Opt. Lett. **20,** 848 (1995).
13. M. D. Duncan, R. Mahon, L. L. Tankerley, and J. Reintjes, J. Opt. Soc. Am. B **5,** 37 (1988).
14. M. D. Duncan, R. Mahon, L. L. Tankerley, and J. Reintjes, J. Opt. Soc. Am. B **7,** 1336 (1990).
15. M. D. Duncan, R. Mahon, L. L. Tankerley, and J. Reintjes, Opt. Lett. **16,** 1868 (1991).
16. J. A. Moon, R. Mahon, M. D. Duncan, and J. Reintjes, Opt. Lett. **19,** 1234 (1994).
17. E. E. Hagenlocker, R. W. Minck, and W. G. Rado, Phys. Rev. **154,** 226 (1967).
18. Q. Z. Wang, P. P. Ho, and R. R. Alfano, in *The Supercontinuum Laser Source*, R. R. Alfano, ed. (Springer-Verlag, New York, 1989), pp. 41–49.